

Case Report

A case of spontaneous Zymbal's gland carcinoma with lung metastasis in an aged Fischer 344 rat

Ai Maeno¹, Yoshimitsu Sakamoto¹, Motoki Hojo^{1*}, Yukie Tada¹, Jin Suzuki¹, Akiko Inomata¹, Takako Moriyasu¹, Akihiko Hirose², Noriko Kemuriyama³, Katsuhiko Miyajima³, and Dai Nakae^{3*}

¹ Department of Pharmaceutical and Environmental Sciences, Tokyo Metropolitan Institute of Public Health, 3-24-1 Hyakunincho, Shinjuku, Tokyo 169-0073, Japan

² Center for Biological Safety and Research, National Institute of Health Sciences, 3-25-26 Tonomachi, Kawasaki Ward, Kawasaki, Kanagawa 210-9501, Japan

³ Department of Nutritional Science and Food Safety, Faculty of Applied Biosciences, Tokyo University of Agriculture, 1-1-1 Sakura-ga-Oka, Setagaya, Tokyo 156-8502, Japan

Abstract: Zymbal's gland neoplasms are induced in rats through the administration of various carcinogens, but spontaneous neoplasia is rare. This report describes a spontaneous Zymbal's gland carcinoma with lung metastasis found in an aged male Fischer 344 rat. Macroscopically, the dome-like tumor nodule, approximately 30 mm in diameter with ulceration, was located near the ear canal of the rat. No healthy tissue or structure of Zymbal's gland was identified on the corresponding side, while the normal salivary glands and a lacrimal gland were observed. Histologically, a large part of the tumor mass was occupied by poorly differentiated neoplastic cells, the shapes of which were oval to polygonal or fusiform. Additionally, clusters of sebaceous-like foamy cells and squamous metaplasia with prominent keratinization were observed. Tumor cells were found to metastasize to the lung; these cells displayed histological similarities, including a sebaceous gland-like pattern, to those in the primary site. The tumor cells were immunohistochemically positive for cytokeratin AE1/AE3 or vimentin but negative for CD68, S100, α -smooth muscle actin, von Willebrand factor, and desmin. Our results indicate that the tumor was a poorly differentiated Zymbal's gland carcinoma with lung metastasis. (DOI: 10.1293/tox.2021-0013; J Toxicol Pathol 2021; 34: 353–358)

Key words: Zymbal's gland, carcinoma, rat, metastasis, lung

Zymbal's gland neoplasms can be induced in rats by the administration of several carcinogenic agents, such as aromatic amines and polycyclic aromatic hydrocarbons. Meanwhile, spontaneous neoplasms of Zymbal's glands are uncommon in rats, regardless of the strain. Large-scale historical data analyses of Fischer 344 (F344) rats have indicated that the incidence of Zymbal's gland tumors is 1.4% (range: 0–8) and 0.7% (0–6) in males and females, respectively¹. Zymbal's gland carcinomas are known to metastasize to the brain, lung, eye, pituitary gland, and liver in aged Sprague–Dawley rats². However, metastases of this tumor to the regional lymph nodes or lungs in F344 rats are relatively rare, and their histopathological conditions have not

been sufficiently characterized¹. Here, we encountered a case of poorly differentiated Zymbal's gland carcinoma with lung metastasis and have described its histopathological and immunohistochemical features.

The animal was a male F344 rat sourced from Charles River Laboratories Japan, Inc. (Kanagawa, Japan), and used in a 2-year carcinogenicity study for multi-walled carbon nanotube (MWCNT)³. The animal was of 10 weeks of age at the start of the study. It was provided with a basal diet, CE-2 (CLEA Japan, Inc., Tokyo, Japan) and tap water *ad libitum*, and housed in a polycarbonate cage (3 rats per cage) in a room maintained at a temperature of 23 ± 0.2 °C (mean \pm standard deviation) and $49.9 \pm 5\%$ relative humidity on a 12 h light–dark photophase cycle. The animal was found in the group dosed with a single intraperitoneal injection of MWCNT at 0.05 mg/kg body weight.

The tumor raised as a firm nodule just under the ear canal on the right side. At first, the skin was freely movable over the nodule, but as the tumor rapidly enlarged, the surface of the tumor adhered to the skin and gained an ulcerative appearance. A blackish mass was first visible at the age of 63 weeks; it looked like a dome and slightly hard and was of size $12 \times 12 \times 4$ mm. When the rat was euthanized

Received: 2 March 2021, Accepted: 8 July 2021

Published online in J-STAGE: 23 July 2021

*Corresponding authors: M Hojo

(e-mail: motoki_hojo@member.metro.tokyo.jp) and

D Nakae (e-mail: agalennde.dai@nifty.com)

©2021 The Japanese Society of Toxicologic Pathology

This is an open-access article distributed under the terms of the Creative Commons Attribution Non-Commercial No Derivatives

(by-nc-nd) License. (CC-BY-NC-ND 4.0: <https://creativecommons.org/licenses/by-nc-nd/4.0/>).



at 77 weeks of age, the size of the tumor mass reached 40 × 30 × 30 mm, and the tumor spread to the muscles of the head (Fig. 1A). A cut surface of the tumor showed white to yellowish-white solid mass with a necrotic area at the center. Macroscopically, no healthy tissue or structure of Zymbal's gland was identified on the side where the tumor arose, but normal salivary glands and a lacrimal gland were visible. In the lung, some white translucent nodules of 1–3 mm size were noted (Fig. 1B). This rat concurrently developed a spontaneous large granular lymphocytic leukemia (LGL) and a peritoneal mesothelioma induced by the MWCNT both of which were confirmed macroscopically and histologically (data not shown). The animal experiments were approved by the Animal Experiment Committee of the Tokyo Metropolitan Institute of Public Health.

The tumor mass was excised, fixed in 10% neutrally buffered formalin, embedded in paraffin, sectioned (thickness: 4–7 μm), and stained with hematoxylin and eosin. For immunostaining, antigen retrieval was performed in 10 mM citrate buffer (pH 6.0) or Tris-EDTA buffer (pH 9.0) using a microwave for 15 min, followed by the inactivation of endogenous peroxidase by immersion in H₂O₂. After blocking, the sections were treated with the following primary antibodies: adipophilin (610102, Progen, Heidelberg, Germany; 1:100 dilution), α-smooth muscle actin (αSMA; M0851, DAKO, Glostrup, Denmark; 1:100), CD68 (ab125212, Abcam, Cambridge, UK; 1:1000), cytokeratin AE1/AE3 (MAB3412, Millipore, Billerica, MA, USA; 1:100), cytokeratin 5 (CK5; ab53121, Abcam; 1:100), desmin (IS606, DAKO; 1:1), S100 (IS504, DAKO; 1:1), SP-C (sc-13979, Santa Cruz Biotechnology, Santa Cruz, CA, USA; 1:100), vimentin (IS63030, DAKO; 1:1), or von Willebrand factor (VWF; ab6994, Abcam; 1:100). Diaminobenzidine signals were detected using the EnVision System (K5361, DAKO) according to the manufacturer's instructions. Also, Oil Red O staining was performed on formalin-fixed frozen sections.

Histological analysis revealed that the neoplasm appeared advanced, showing not only external expansion but also aggressive invasion, or infiltration into the surrounding tissues (i.e., muscles and the ear canal) without capsules (Fig. 2A). The tumor cells invaded the temporal muscle, but not the cranial bone or brain. Despite intensive histological sample preparations, unaffected Zymbal's gland tissues were not observed apart from the tumor mass on the side of the tumor. Although small clusters of sebaceous gland-like foamy cells were widely scattered in the tumor, especially in the center of the mass (Fig. 2B), a large part of the lesion consisted of highly pleomorphic cells with hyperchromatic nuclei that formed versatile histological patterns. For instance, the tumor contained giant, multinuclear, or unusually shaped cells with numerous mitotic figures (Fig. 2C and 2D). The tumor cells could be roughly classified into 2 types: oval-to-polygonal cells with epithelial characteristics and spindle-shaped cells with mesenchymal properties. Each cell type was mixed irregularly throughout the lesion. The representative structures formed by the epithelial-type cells included a solid sheet (Fig. 2E) and squamous epithelium-like pro-

liferation (Fig. 2F). Prominent squamous metaplasia with a high degree of keratinization was observed in the vicinity of the epidermis (Fig. 2G). Conversely, the mesenchymal-type cells exhibited a sheet or bundle-like growth pattern (Fig. 2H). Furthermore, these 2 types of cells appeared to transition to each other in some areas (Fig. 2I). Immunohistochemically, they were mutually positive for cytokeratin AE1/AE3 or vimentin (Fig. 3A to 3C), corresponding to the polygonal cells or fusiform cells, respectively. Both cell types were negative for cytokeratin 5, S100, αSMA, CD68, VWF, and desmin. Sebaceous gland-like cells were positive for cytokeratin AE1/AE3 and adipophilin (Fig. 3D–3F) but negative for vimentin (Fig. 3E, inset). Additionally, cytokeratin 5 positivity was found in some small cells surrounding the sebaceous gland-like tumor cells, which may be stromal and/or supporting cells functionally associated with Zymbal's gland cells. Lastly, Oil Red O staining did not reveal clearly recognizable fat droplets in the cytoplasm of the tumor cells (data not shown).

In accordance with the macroscopic finding of the lung, multifocally proliferative nodules were observed in the parenchyma (Fig. 4A). Some epithelial-type cells exhibited sebaceous-like patterns in which several oval cells with small nuclei and highly foamy cytoplasm formed a lobular architecture similar to the intact Zymbal's gland acinar (Fig. 4B). Immunohistochemical analysis showed that the tumor cells were negative for CD68, SP-C, and cytokeratin 5, suggesting the growth of some translocated tumor cells. Intriguingly, like the buccal tumor, the proliferated cells could be approximately divided into 2 populations, epithelial- and mesenchymal-type cells that corresponded to the cytokeratin AE1/AE3-positive and vimentin-positive cells, respectively (Fig. 4C–4E). Sebaceous-like cells were positive for cytokeratin AE1/AE3 as well as adipophilin (Fig. 4F–4H). Similar to the buccal tumor, these sebaceous-like cells were surrounded by small cytokeratin 5-positive cells (data not shown). In addition, at a site deep in the parenchymal region, metastatic cell extravasation was observed, and the tumor cells had destroyed a blood vessel wall (Fig. 4I). The tumor cells in and around the blood vessel were spindle-shaped and immunohistochemically only positive for vimentin (Fig. 4J and 4K). These observations suggested that the primary site might be the Zymbal's gland, and metastasis might have occurred. Metastatic cells were not detected in regional lymph nodes, such as the submandibular lymph node. We have experienced that peritoneal mesotheliomas induced by MWCNTs could translocate to the mediastinal lymph node and the lungs, and they are usually sarcomatoid-type cells and stained with anti-vimentin antibody (our unpublished data). Nonetheless, in this rat, mesothelioma is believed to be early stage. In other words, small nodules largely comprising epithelioid-type cells were sparsely detected in the serosa of the abdominal organs, and no invasion was observed (data not shown), indicating that metastasis was unlikely. A possibility about the infiltration of LGL tumor cells is also unlikely because of their cellular morphology.

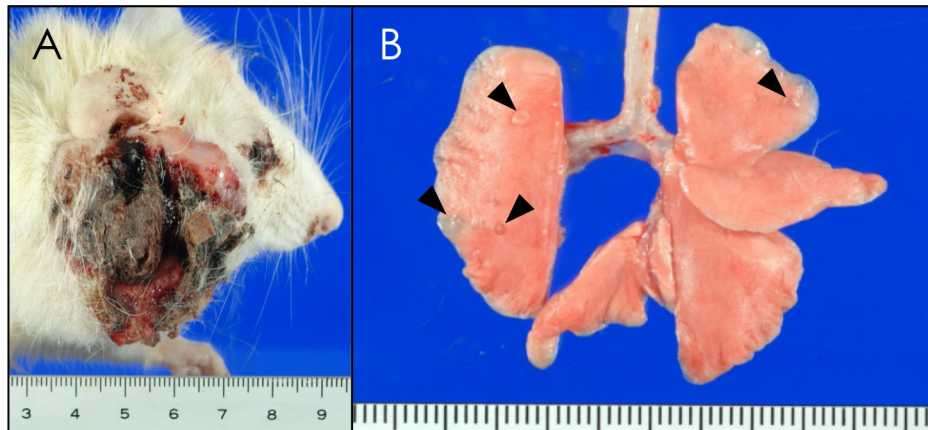


Fig. 1. Macroscopic analysis of the primary and metastatic Zymbal's gland tumor. The tumor developed on the right side of the buccal surface. The surface of the tumor was ulcerated and covered with a dry, blackish crust (A). Additionally, several white translucent nodules with a diameter of 1–3 mm (arrowheads) were observed in the lung parenchyma (B).

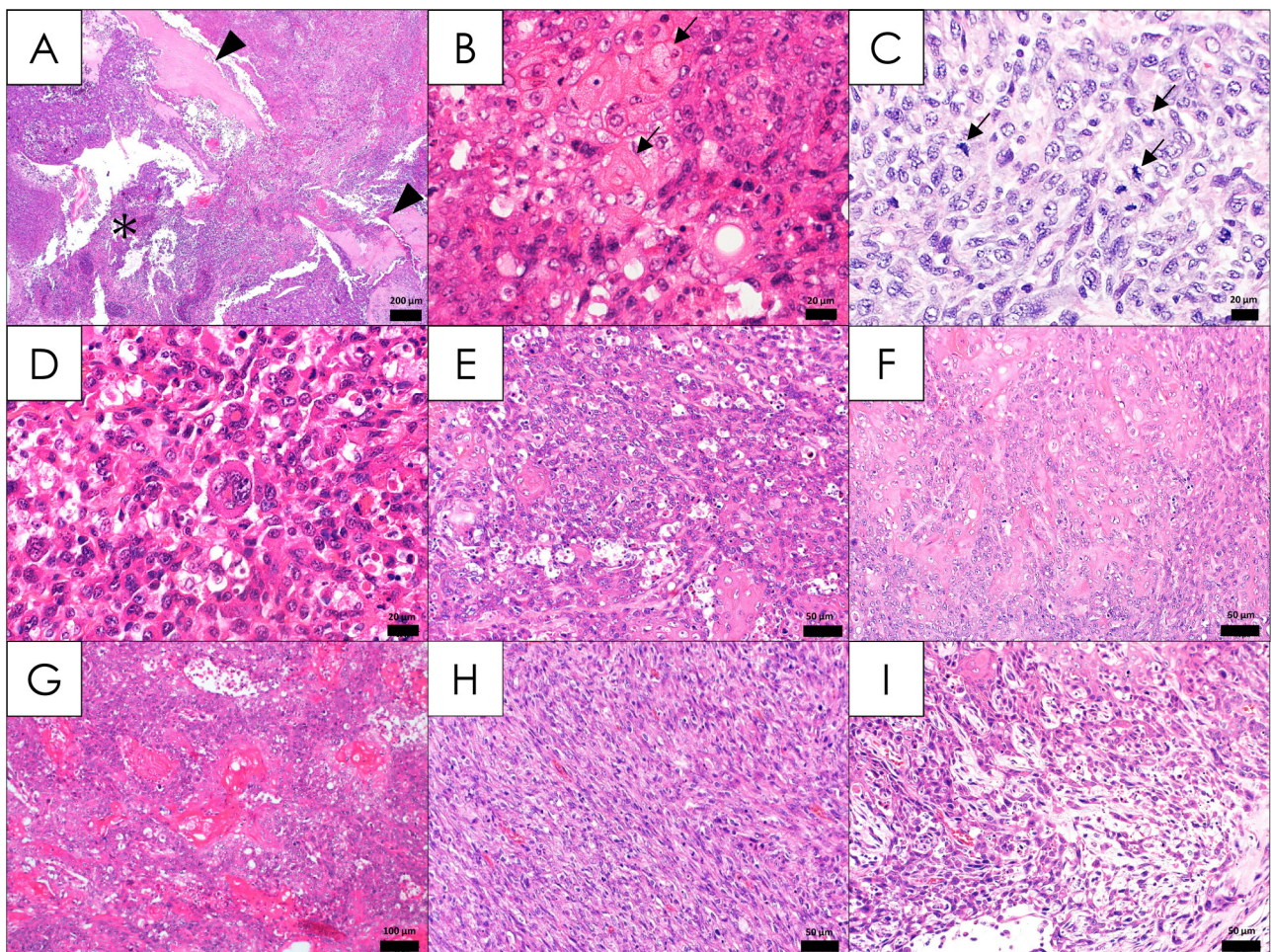


Fig. 2. Representative histology of the tumor by hematoxylin and eosin staining. Neoplastic cells were arranged irregularly, with hemorrhage and necrosis beneath the epidermis. The tumor cells destroyed bones (arrowheads) and infiltrated the external auditory canal (asterisk) (A). The sebaceous gland-like foamy cells (arrows) are usually necrotic or degenerative and surrounded by more atypical tumor cells (B). The neoplasm consisted of various cell shapes, such as highly pleomorphic cells with mitoses (C; arrows), giant cells, and multinuclear cells (D). The epithelial-type tumor cells varied in appearance, from oval to polygonal cells, forming a solid sheet (E) to squamous epithelium-like cells (F), often accompanied by marked keratinization (G). Mesenchymal-type tumor cells formed a bundle-like pattern (H). Finally, epithelial-type tumor cells transitioned to mesenchymal cells (I).

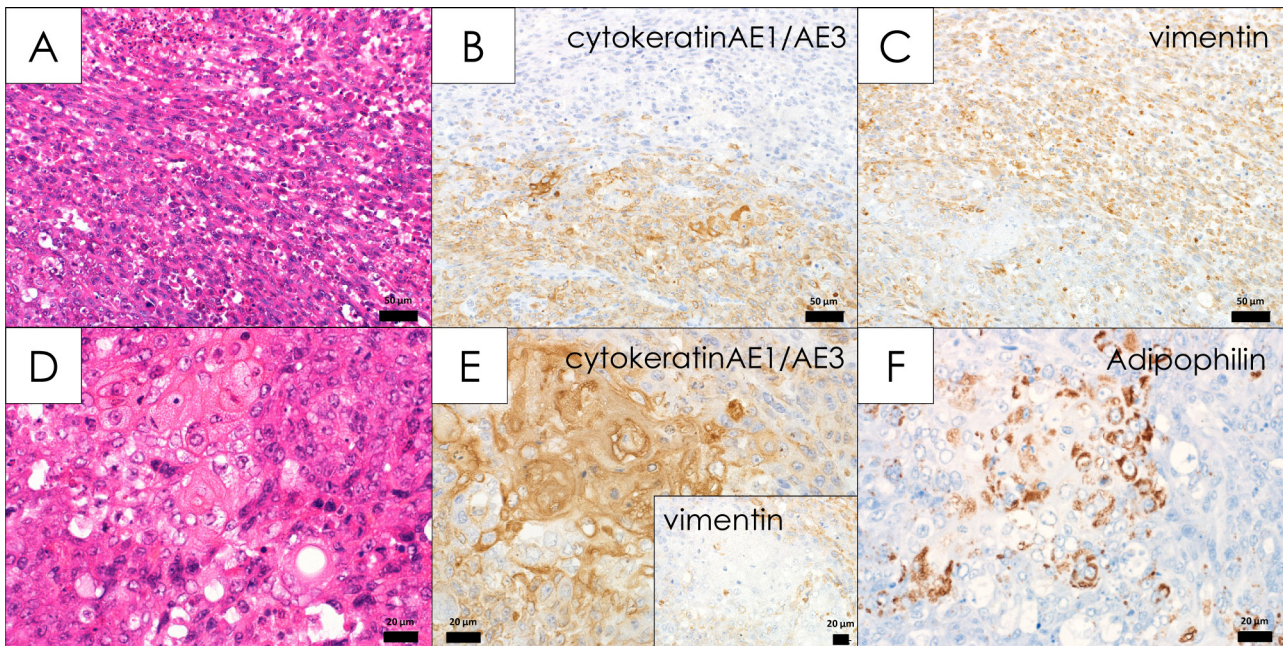


Fig. 3. Immunohistochemical staining of the tumor cells. The epithelial-type (A, lower half) and mesenchymal-type (A, upper half) tumor cells were positive for cyokeratin AE1/AE3 (B) and vimentin (C), respectively. The sebaceous gland-like cells (D) were positive for cyokeratin AE1/AE3 (E) but negative for vimentin (E, inset). In addition, the adipophilin positivity was confined to these cells (F).

Judging from these results, the tumor was diagnosed as a Zymbal's gland carcinoma exhibiting a poorly differentiated status and lung metastasis. Although the continuity of the tumor to a distinguishable intact tissue was not observed, the morphological and immunohistochemical features of sebaceous gland cells, the findings of the tumor location, and the rapid growth with ulceration suggested that this neoplasm arose from Zymbal's gland. Thus, the existing Zymbal's gland was likely replaced by tumor tissues.

Generally, Zymbal's gland tumors originate from both the sebaceous gland and ductal epithelium; thus, the usual carcinomas are diagnosed as a sebaceous cell subtype or squamous cell subtype. Regardless of the subtype, the 2 types of cells are usually mixed at varying proportions^{1, 4}. Meanwhile, carcinoma often consists of atypical tumor cells and lacks normal acinar and ductal structures. It is believed that some poorly differentiated cases are solid masses formed by atypical spindle-shaped cells accompanied by stroma that resembles carcinosarcoma⁵.

We propose that the tumor in the present case likely originated from sebaceous gland cells and entered an anaplastic and undifferentiated state as the tumor progressed, resulting in a mesenchymal or epithelial feature depending on its microenvironment. Since metastasis is generally driven by the epithelial-mesenchymal transition of tumor cells, metastasis appeared to occur easily in this case. Indeed, the mesenchymal status of the tumor was demonstrated in the blood vessels of the lung parenchyma. Our case was derived from an MWCNT-exposed group. However, it was unlikely

that this tumor was related to the administration of MWCNTs because of the low incidence; it was not significantly elevated compared with the control group in the carcinogenicity study, and MWCNT fibers were not detected around the tumor. To the best of our knowledge, there are no reports available on the toxicological effects of MWCNTs on Zymbal's glands^{6, 7}. The Zymbal's gland has been reported as a target of various carcinogens. The susceptibility of this tissue to chemical-induced tumors may be attributed to the activities of the gland with respect to converting lipophilic chemicals to more reactive metabolites, although the mechanism remains elusive. Our histological analysis, especially the features of the metastatic cells in the lung, is expected to be useful for understanding the pathogenesis of Zymbal's gland carcinoma and for developing precise diagnosis in future carcinogenic studies.

Disclosure of Potential Conflicts of Interest: The authors declare there are no conflicts of interest.

Acknowledgments: This study was funded in part by a Health and Labor Sciences Research Grant (H27-Kagaku-Shitei-004 and H30-Kagaku-Shitei-004) from the Ministry of Health, Labour and Welfare of Japan. We are grateful to Katsuhiro Yuzawa, Akemichi Nagasawa, the late Yoshikazu Kubo, Fujifumi Kaihoko, Kyoko Hiramatsu, Yuko Hasegawa, Norio Yano, Hiroshi Ando, and Kazuyoshi Tanaka for their superb technical supports.

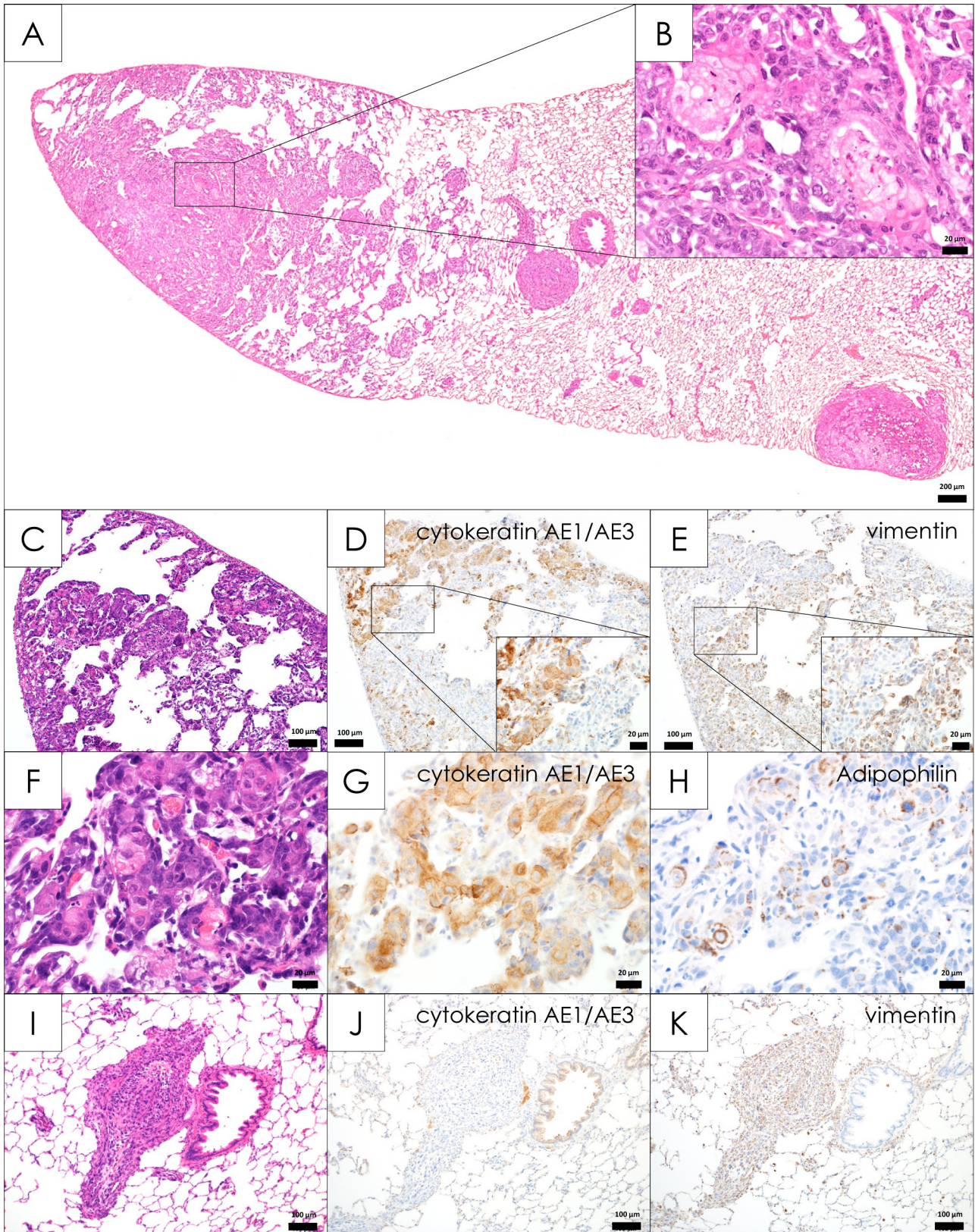


Fig. 4. Representative histology of the metastatic sites in the lung. Multifocal nodules without clear boundaries were observed between the neoplastic cells and parenchymal tissues (A). Some epithelial-type cells exhibited sebaceous gland-like patterns (B). In a serial section of A (C), the two types of tumor cells were distinguished by immunohistochemical staining with cytokeratin AE1/AE3 (D) and vimentin (E). The sebaceous gland-like cells (F) were positive for cytokeratin AE1/AE3 (G) and adipophilin (H). The newly arriving metastatic cells in and around a blood vessel (I) were immunohistochemically negative for cytokeratin AE1/AE3 (J) but positive for vimentin (K).

References

1. Copeland-Haines D, and Eustis SL. Specialized sebaceous glands. In: Pathology of the Fischer Rat. GA Boorman, SL Eustis, MR Elwell, CA Montgomery, and WF MacKenzie (eds). Academic Press, San Diego, 279–293. 1990.
2. Chandra M, Riley MG, and Johnson DE. Spontaneous neoplasms in aged Sprague-Dawley rats. *Arch Toxicol.* **66**: 496–502. 1992. [[Medline](#)] [[CrossRef](#)]
3. Hojo M, Yamamoto Y, Sakamoto Y, Maeno A, Ohnuki A, Suzuki J, Inomata A, Moriyasu T, Taquahashi Y, Kanno J, Hirose A, and Nakae D. Histological sequence of the development of rat mesothelioma by MWCNT, with the involvement of apolipoproteins. *Cancer Sci.* **112**: 2185–2198. 2021. [[Medline](#)] [[CrossRef](#)]
4. Yoshizawa K. Specialized sebaceous glands—Zymbal's gland, preputial gland, clitoral gland, and perianal gland. In: Boorman's Pathology of the Rat, 2nd ed. GA Boorman, AW Suttie, JR Leininger, SL Eustis, MR Elwell, AE Bradley, and WF MacKenzie (eds). Academic Press, San Diego, 347–365. 2018.
5. Kajimura T. Ear and its accessory glands. In: New Toxicologic Histopathology. The Japanese Society of Toxicological Pathology (ed). Nishimura Shoten, Tokyo, 585–595. 2017.
6. Kasai T, Umeda Y, Ohnishi M, Mine T, Kondo H, Takeuchi T, Matsumoto M, and Fukushima S. Lung carcinogenicity of inhaled multi-walled carbon nanotube in rats. *Part Fibre Toxicol.* **13**: 53. 2016. [[Medline](#)] [[CrossRef](#)]
7. Suzui M, Futakuchi M, Fukamachi K, Numano T, Abdelgied M, Takahashi S, Ohnishi M, Omori T, Tsuruoka S, Hirose A, Kanno J, Sakamoto Y, Alexander DB, Alexander WT, Jiegou X, and Tsuda H. Multiwalled carbon nanotubes intratracheally instilled into the rat lung induce development of pleural malignant mesothelioma and lung tumors. *Cancer Sci.* **107**: 924–935. 2016. [[Medline](#)] [[CrossRef](#)]